Unusual Coordination Behavior of Cr^{3+} in Microporous Aluminophosphates

Andrew M. Beale,[†] Didier Grandjean,[†] Jan Kornatowski,[‡,§] Pieter Glatzel,[†] Frank M. F. de Groot,[†] and Bert M. Weckhuysen*[,†]

Department of Inorganic Chemistry and Catalysis, Debye Instituut, University of Utrecht, Sorbonnelaan 16, 3584 CA Utrecht, The Netherlands, Max-Planck Institut für Kohlenforschung, 45470 Mülheim/Ruhr, Germany, and Faculty of Chemistry, Nicholas Copernicus University, 87-100 Torun, Poland

Received: June 9, 2005; In Final Form: November 15, 2005

A CrAPO-5 molecular sieve has been investigated with X-ray absorption spectroscopy (EXAFS-XANES) as dehydrated material and after loading with water and ammonia to unravel the coordination geometries of Cr^{3+} in the framework of a microporous crystalline aluminophosphate, more particularly of the AFI-type. A comparison of the XANES data, a preedge analysis with crystal field multiplet calculations and EXAFS data, pointed toward the presence of framework Cr^{3+} which, on dehydration, takes on a distorted tetrahedral coordination state. Due to the $3d^3$ configuration of Cr^{3+}, this unusual tetrahedral coordination environment strongly tends to transform into the more stable 6-fold coordination geometry by binding two extraframework water molecules during hydration. In the presence of ammonia, tetrahedral Cr^{3+} readily transforms into a 5-fold coordination geometry by binding one ammonia molecule. Therefore, depending on the environmental conditions, the Cr^{3+} ions can occur in a 4-, 5-, or 6-fold coordination. This observation underlines the flexibility of transition metal ions, such as Cr^{3+}, to cope with unusual coordination geometries in inorganic hosts, making them interesting as potential active sites in heterogeneous catalysis.

Introduction

Cr^{3+} in inorganic compounds exhibits a strong tendency to adopt octahedral coordination. The reason is the stability of the trivalent ion and its $3d^3$ $^4A_2$ ground state with all t_{2g} spin-up states filled. The binary oxide Cr_2O_3 is far more stable than the Cr^{4+} system CrO_2, while the Cr^{2+} oxide CrO is the only form of transition metal monoxide that does not exist, at least in a bulk form. Cr^{3+} in tetrahedral coordination is very rare.[1,2] Using UV−Vis−NIR spectra, tetrahedral Cr^{3+} has been shown to exist in systems such as Cr-bearing blue-colored diopsides, Cr-heteropolytungstate, Na_4CrO_4, and Cr[μ_3-O_4] cubanes.[3−7] In inorganic bulk oxides, tetrahedral Cr^{3+} has been claimed a few times but without clear spectroscopic proof.[8,9] One of the problems is the potential coexistence of other oxidation states of Cr in the materials under study, making the spectroscopic fingerprinting of tetrahedral Cr^{3+} far from unambiguous.

Microporous aluminophosphate molecular sieves have a crystalline three-dimensional network, in which aluminum and phosphorus tetrahedra are linked via oxygen atoms. The framework Al or P atoms can be replaced by other elements, such as transition metals, in a process called isomorphous substitution, leading to materials with modified adsorption and catalytic properties.[9,10] Although isomorphous substitution implies a tetrahedral coordination of the guest ion, molecular sieves are more flexible than is often thought, since it is possible for the substituent to adopt other coordination states. For example, a number of molecular sieves exist in which Al^{3+} ions can possess octahedral coordination, in the presence of water.[11] Thus, aluminophosphates as well as other zeolitic materials should be ideal hosts to accommodate the unusual tetrahedral-like Cr^{3+} environment. As a consequence, many attempts have been reported to synthesize Cr-containing microporous crystalline aluminophosphates, CrAPO-5 being the most prominent material.[12,13] Unfortunately, spectroscopic analyses of these materials always pointed toward the presence of octahedral-like Cr^{3+}, which was taken as a proof for the existence of extraframework chromium. Other characterization techniques revealed that the chromium ions either really occurred in extraframework species or were incorporated in an unstable manner (cf. ref 14c and references therein). A stable incorporation of Cr^{3+} became possible with a new synthesis procedure applied for CrAPO-5.[14] It was demonstrated that a large portion of the Cr^{3+} ions was actually incorporated into the framework tetrahedral sites. Although a model for the Cr^{3+} bonding and coordination changes has been proposed,[14c] a detailed insight in the coordination environment of Cr^{3+} has not been evidenced.

The goal of this work is the detailed spectroscopic characterization of the coordination environment of Cr^{3+} in CrAPO-5 material both in the dehydrated and the hydrated or ammonia saturated states. The technique of X-ray absorption spectroscopy (EXAFS-XANES) has been chosen since it allows assessing the oxidation state, coordination number, and bond lengths of framework Cr^{3+}. It will be shown that (1) Cr^{3+} ions occupy a 4-fold coordination in the aluminophosphate framework after dehydration and (2) the tetrahedral-like Cr^{3+} guest ion significantly distorts the framework host. Tetrahedral-like framework Cr^{3+} readily coordinates two "extraframework" water molecules as additional ligands under ambient conditions. In the case of ammonia, coordination of one ammonia molecule occurs giving rise to a 5-fold coordination environment for Cr^{3+}.

Experimental Section

The preparation method of CrAPO-5 materials has been described in detail elsewhere and the sample used for the present measurements had a Cr content of 0.321 mmol/g or 1.67 wt

* To whom correspondence should be addressed. E-mail: b.m.weckhuysen@chem.uu.nl.
† University of Utrecht.
‡ Max-Planck Institut für Kohlenforschung.
§ Nicholas Copernicus University.

10.1021/jp0531006 CCC: $33.50
Published on Web 12/16/2005

%.[14] The pretreatment of the solid prior to the spectroscopic measurements was done in specially designed cells to prevent sample contamination and potential hydration. Dehydration was carried out by heating the calcined sample at a rate of 1 deg/min to 300 °C in He and keeping it at this temperature for 1 h. Rehydration was performed at 120 °C for 30 min, using a water-saturated He stream. Saturation with ammonia of CrAPO-5 was done on a dehydrated sample by passing ammonia flow over the material at 90 °C for 30 min. XAS measurements were carried out in situ at 300 °C for the dehydrated material and after cooling the material at room temperature in the same atmosphere used for the treatment, for the materials rehydrated and saturated with ammonia. UV−Vis−NIR experiments in the diffuse reflectance mode were conducted at room temperature with a Varian Cary 500 spectrometer with $BaSO_4$ as a white reference standard. X-ray absorption data were collected on beamline E4 of Hasylab (DESY, Hamburg, Germany) operating under beam conditions of 4.4 GeV and 150 mA, using a Si(111) double-crystal monochromator. Self-supporting wafers were measured in fluorescence mode with a 9-channel Ge detector at the Cr K edge (5989.2 eV). Acquisition times were typically less than 8 min for XANES and up to 40 min for EXAFS with energy resolution of 0.3 to 2 eV and 2 to 5 eV for XANES and EXAFS measurements, respectively.

Data reduction and EXAFS refinements were performed with the programs EXBROOK and EXCURV98, respectively.[18] Phase shifts and backscattering factors were calculated with ab initio techniques, using Hedin−Lundqvist potentials. Refinements were carried out by using k^3 weighting in the range 3.5−12.5 Å for the de- and re-hydrated materials and 3.6−10.0 Å for the ammonia saturated one. Fourier transform peaks were isolated with a Gaussian window (1.0−3.6 Å) and the contribution of this group of shells was extracted by inverse transformation. The AFAC factor (amplitude reduction due to many-electron processes) calibrated from the fit of a Cr metal foil was fixed at 0.85.

After normalization with the EXBROOK program, the contribution of the edge jump to the preedge was modeled by a combination of one ascending Gaussian cumulative and pseudo-Voigt components, using the software Peakfit 4.0. After subtraction of the edge jump, the preedges were fitted with pseudo-Voigt functions to derive normalized height, position, and width. To subtract the contribution of the Cr^{6+}, the preedge was fitted with two pseudo-Voigt components: one at a fixed energy of 5993.6 eV and with a fixed width (simulating Cr^{6+}) and a second one that was allowed to vary. The component at fixed energy was then subtracted from the experimental curve.

Results and Discussion

The UV−Vis−NIR diffuse reflectance spectrum of as-synthesized green-colored CrAPO-5 is characterized by absorption bands at 15 900 and 21 800 cm^{-1}. These bands are due to the ν_1 and ν_2 transitions of Cr^{3+} in (pseudo-) octahedral coordination.[14c,15] Calcination of this material in air at 500 °C for 12 h turns the material to yellowish-green and two new absorption bands, besides the Cr^{3+} d−d transitions, are observed at 27 000 and 37 000 cm^{-1}. These bands are the charge-transfer transitions of Cr^{6+}, formed by oxidation of part of Cr^{3+} during calcination.[14c,15] Dehydration at 350 °C for 12 h in He results in a color change from yellowish-green to purple-blue and the corresponding spectrum is shown in Figure 1. The spectrum is dominated by three broad absorption bands at 8 400, 14 500, and 20 300 cm^{-1}. Table 1 shows that these values are close to those of the diopside mineral[4] and the Cr-heteropolytungstate.[5]

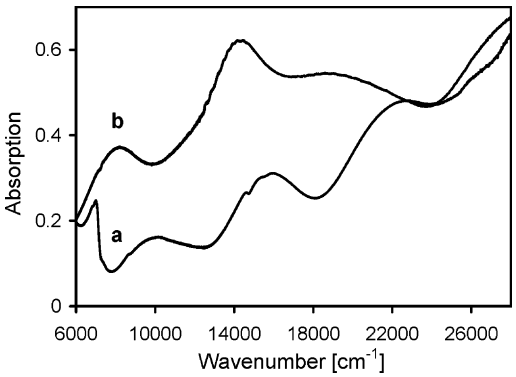

Figure 1. UV−Vis−NIR diffuse reflectance spectra of hydrated (a) and dehydrated (b) CrAPO-5 molecular sieves.

TABLE 1: UV−Vis−NIR Band Positions (cm^{-1}) of Hydrated and Dehydrated CrAPO-5 Molecular Sieves Compared with Tetrahedral Cr^{3+} Systems

tetrahedral $^4T_1$				
Cr-diopside[4]	9 170	13 550	17 150	22 830
Cr-heteropolytungstate[5]	8 300	16 000	19 200	
dehydrated CrAPO-5	8 400	14 500	20 300	
octahedral $^4A_2$				
hydrated or rehydrated CrAPO-5	15 900	21 800	27 000[a]	37 000[a]

[a] The bands at 27 000 and 37 000 cm^{-1} correspond to charge-transfer transitions of Cr^{6+}.

It is important to notice that the former band has never been reported for this material in the literature most probably due to instrumental limitations and problems of sample hydration.[14] Rehydration of CrAPO-5 results in a color change to yellowish-green and absorption bands at about 16 000 and 22 800 cm^{-1} become visible. Such hydration−dehydration cycles give reproducible effects.[14]

The study of the Cr K-edge X-ray absorption spectra has been focused on the evidence for tetrahedral Cr^{3+} by analyzing more specifically the preedge structures and the EXAFS region of the spectra. XANES spectra of hydrated and dehydrated CrAPO-5 presented in Figure 2a are both located at ca. 6000.0 eV, which is characteristic of Cr^{3+}, and feature different profiles indicating different Cr environments. The analysis of the normalized preedge region around 5992 eV is more informative than the study of the Cr K-edge itself since it provides very accurate information on the valence and the local geometry of the metal site. Indeed, the energy position of the centroid of the two preedge features correlates with the Cr valence while the integrated intensity of these features correlates with the local geometry with the largest intensity for tetrahedrally coordinated atoms.[16,17] Figure 2b shows the normalized and background subtracted preedge spectra of hydrated and dehydrated CrAPO-5. The preedge spectrum of the as-prepared CrAPO-5 (spectrum b) is characterized by two small preedge features located at 5990.8 and 5993.4 eV, where Cr in this sample occurs as Cr^{3+} in 6-fold coordination. The preedge spectrum of hydrated CrAPO-5 (spectrum a) is characterized also by two preedge features located at 5990.8 and 5993.2 eV, where the second feature is much more intense. Instead, for dehydrated CrAPO-5 (spectrum c) the centroid is located at 5991.9 eV and the integrated intensity is much larger.

To understand further the structure and origin of these features, preedge structure calculations were performed for chromium with valences 2, 3, 4, and 6 and are shown in Figure 2c. The calculations have been performed with the crystal field multiplet program[19] assuming an ionic ground state and a pure

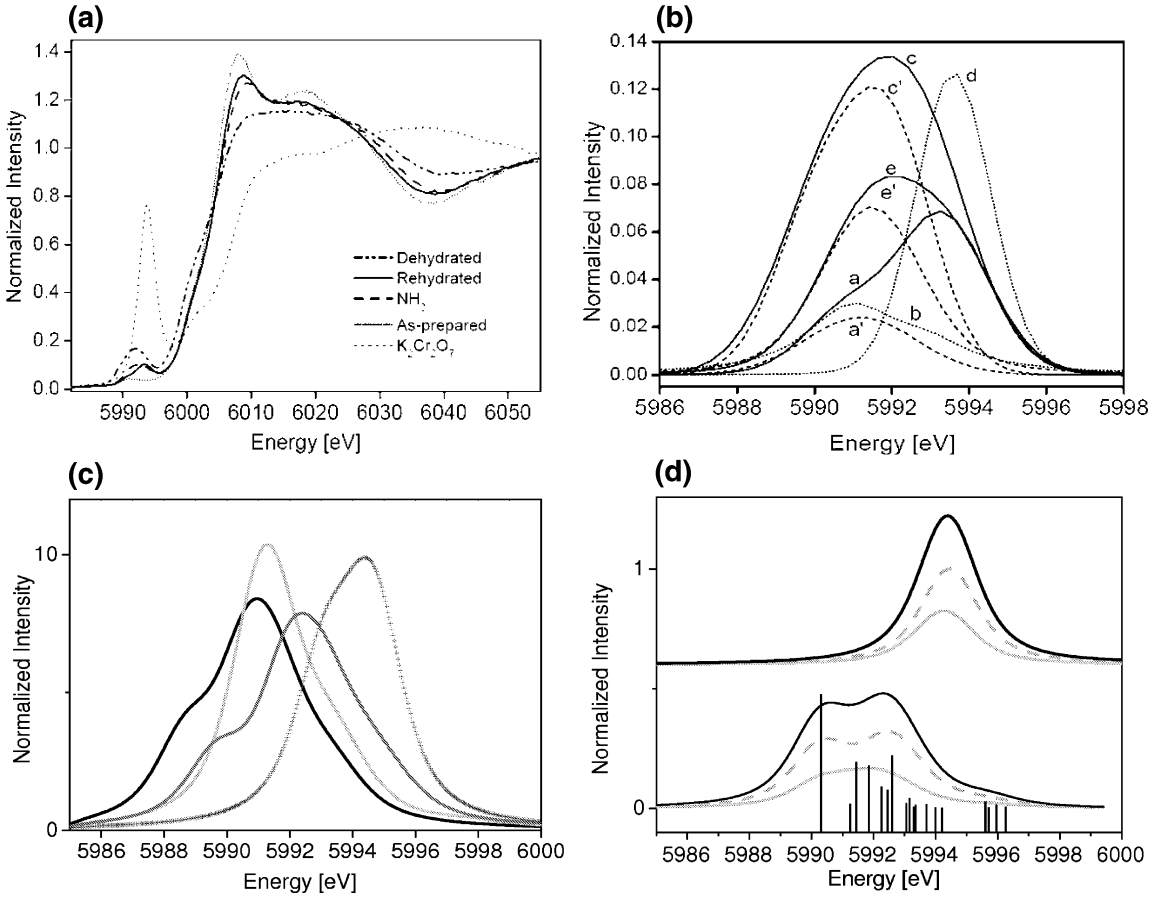

Figure 2. (a) Normalized XANES spectra of as prepared, hydrated, dehydrated, and ammonia saturated CrAPO-5, compared with $K_2Cr_2O_7$. (b) Preedge spectra (after background subtraction) of hydrated (a), as prepared (b), dehydrated (c), and ammonia saturated (e) CrAPO-5, compared with scaled K_2CrO_4 (d). The dotted lines (a′) (c′), and (e′) are the corresponding spectra in which the Cr^{6+} contribution has been eliminated. (c) The quadrupole calculation for Cr^{2+} (solid), Cr^{3+} (light gray), Cr^{4+} (dark gray), and Cr^{6+} (symbols). (d) The total preedge (solid) for Cr^{6+} (top) and Cr^{3+} (bottom). The preedge is divided into dipole (dashed) and quadrupole (solid) calculations. For Cr^{3+} the stick spectrum (before broadening) is added.

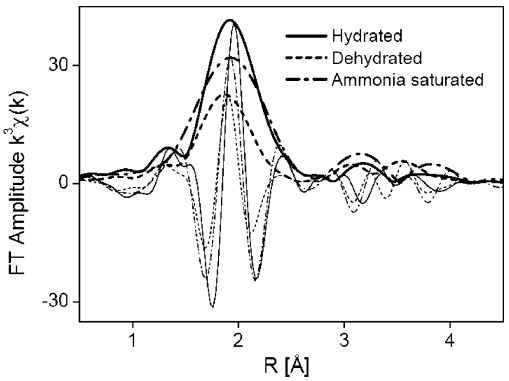

Figure 3. Fourier transforms (FT) of EXAFS spectra (after background subtraction, k^3-weighted) of hydrated, dehydrated, and ammonia saturated CrAPO-5.

quadrupole transition. The Cr^{3+} calculation assumes a $1s^23d^3$ ground state and a $1s^13d^4$ final state. The centers of the respective calculations assume a linear shift with valence of 1 eV/electron. The crystal field values are respectively 1.2 eV for Cr^{2+}, 1.8 eV for Cr^{3+}, and 2.4 eV for Cr^{4+}, typical for octahedral oxide systems. Cr^{6+} has been simulated in tetrahedral symmetry with a crystal field of 1.0 eV. In Figure 2a,b we have seen that the tetrahedral systems have a significantly increased intensity due to the admixture of dipole nature into the quadrupole transitions. This has been simulated in Figure 3b for Cr^{3+} and Cr^{6+}. Cr^{6+} relates to a $1s^23d^0$ ground state and $1s^13d^1$ final state. The $1s^13d^1$ final state is split into its E and T_2 crystal field split states, where only the T_2 state shows quadrupole−dipole mixing. This implies that the quadrupole transition has two peaks, while the dipole admixture has only a single peak. We have estimated the dipole nature to have twice the intensity of the quadrupole intensity. Figure 2d shows the calculation for Cr^{3+} ($3d^3$) in tetrahedral symmetry. All the individual transition intensities are given for the quadrupole transition. Each of these states mixes differently with the dipole transition, which yields the dipole spectrum. After addition of the experimental resolution and the lifetime broadening, the preedge spectra show little remaining structure. Cr^{2+} has a clear satellite at 5988 eV and octahedral Cr^{3+} has an asymmetric spectrum with a tail toward 5994 eV. In contrast, tetrahedral Cr^{3+} has a symmetric preedge structure.

The UV−Vis−NIR data (Table 1) have shown that a small amount of Cr^{6+} exists in both hydrated and dehydrated CrAPO-5, which is confirmed by the preedge data. To remove the Cr^{6+} contribution corresponding to spectrum d (K_2CrO_4 scaled), spectra a and c have been fitted with two peaks (Cr^{3+} and Cr^{6+}) with the broadening of the Cr^{6+} peak set to that of spectrum d. This resulting Cr^{6+} peak has then been subtracted from the preedge spectra. This procedure could introduce some small deviations because the octahedral Cr^{3+} preedge contains some structure at the same energy as Cr^{6+} (cf. Figure 2). The resulting spectra for hydrated CrAPO-5 (spectrum a′) and dehydrated CrAPO-5 (spectrum c′) occur at the same energy, 5990.8 eV for as prepared (spectrum b) and hydrated (spectrum a′) CrAPO-5 and 5990.5 eV for dehydrated (spectrum c′) CrAPO-

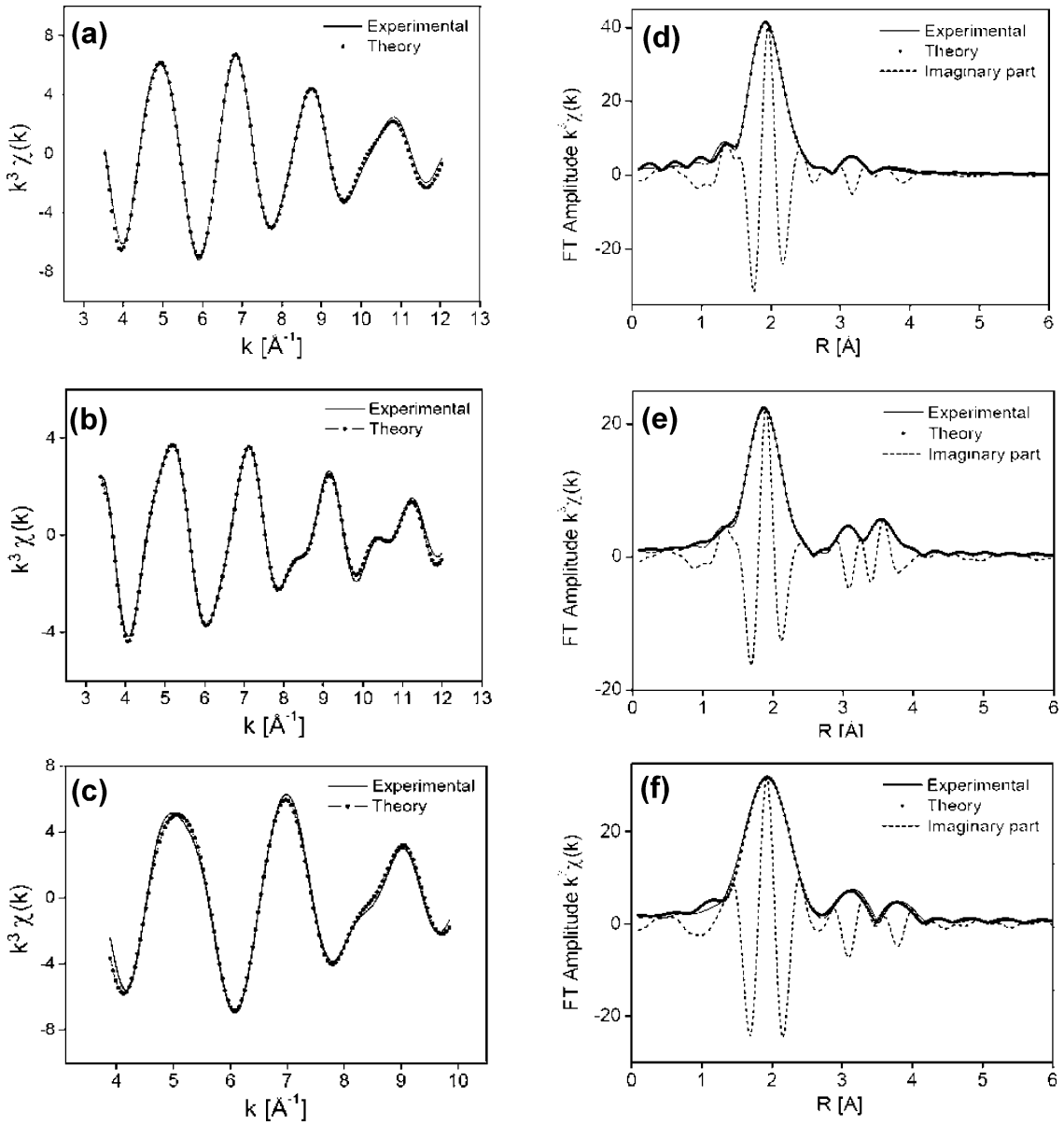

Figure 4. Cr K-edge EXAFS spectra (after background subtraction, k^3-weighted) of hydrated (a), dehydrated (b), and ammonia saturated (c) CrAPO-5 and Fourier transforms of the corresponding EXAFS spectra (d, e, and f). The solid lines are the experimental data and the dotted line is the best fit.

5. This confirms that the valence is essentially maintained at 3+ for all samples. Furthermore, the asymmetric line shape of spectrum a′ is similar to the calculated octahedral Cr^{3+} spectrum, confirming the octahedral nature of the sites. The relative intensities of the preedge of the dehydrated CrAPO-5 (spectrum c′) are approximately 5 times larger than the as-prepared (spectrum b) and hydrated (spectrum a′) samples. This behavior is similar to that observed for $3d^5$ Fe^{3+} systems, where a change in the local coordination state from octahedral to pure tetrahedral symmetry occurs, and can only be explained by an analogous change from an octahedral to a tetrahedral symmetry of the Cr^{3+} ions, although a more intense preedge feature is present for the comparatively electron poor $3d^3$ system due to a greater transition probability.[17] In addition peak c′ is much more symmetric, in line with the theoretical calculations for tetrahedral Cr^{3+} sites. To substantiate this point, an additional measurement has been conducted for dehydrated CrAPO-5 under flow of pure CO at 450° C for 1 h. The result shows that the preedge peak shifts to lower energy (5989.8 eV), indicating formation of Cr^{2+} ions, most likely originating from a partial reduction of Cr^{3+}.[14b]

TABLE 2: EXAFS Results for Hydrated, Dehydrated, and Ammonia Saturated CrAPO-5[a]

sample	scatterer	coord no. N	distance R (Å)	Debye−Waller term $2\sigma^2$ (Å^2)
hydrated	O	4.8	1.96	0.008
CrAPO-5	O	0.9	2.39	0.004
	P	3.1	3.23	0.024
dehydrated	O	3.1	1.89	0.013
CrAPO-5	O	1.0	2.33	0.017
	P	1.0	3.13	0.018
ammonia saturated	O/N	4.0	1.94	0.010
CrAPO-5	O	1.0	2.40	0.007
	P	1.5	3.10	0.003

[a] $AlPO_4$-5 (*P*6*cc*): $a = b = 13.718$ Å, $c = 8.4526$ Å. Al: 1O at 1.718 Å, 1O at 1.713 Å, 1O at 1.732 Å, 1O at 1.672 Å, 2P at 3.089 Å, 1P at 3.119 Å, 1P at 3.143 Å,1 Al at 4.051 Å.[21,22]

The EXAFS results are in good agreement with the preedge analysis and UV−Vis−NIR data. A comparison of the Fourier transforms of the hydrated and dehydrated CrAPO-5 samples (Figure 3) clearly shows that two big changes are affecting the local structure around Cr by dehydration. The first effect is a

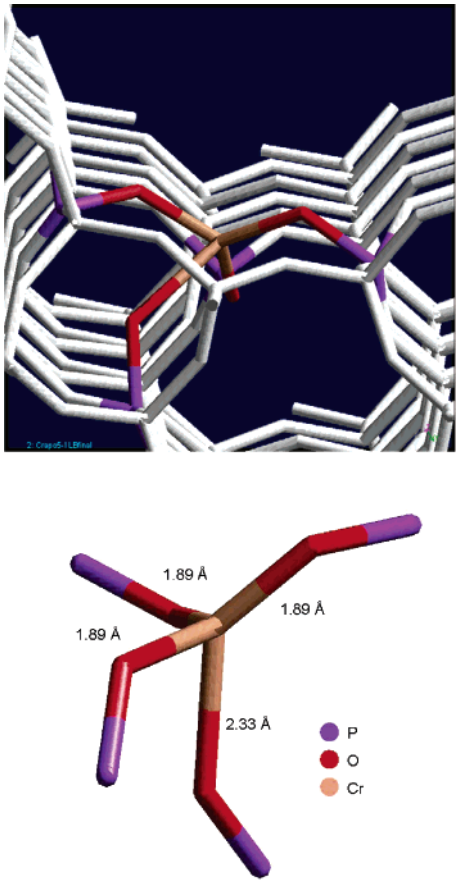

Figure 5. Proposed structural model for the local Cr coordination in dehydrated CrAPO-5.

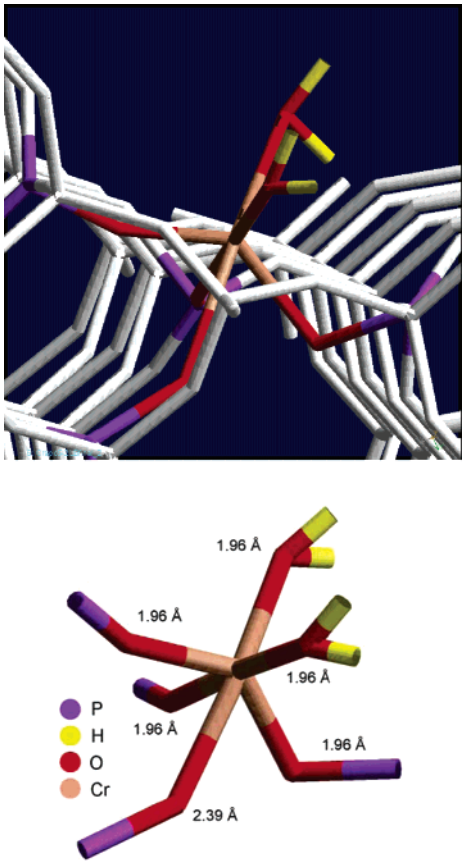

Figure 6. Proposed structural model for the local Cr coordination in hydrated CrAPO-5.

large decrease in the intensity of the broad peak located at around 1.9 Å, corresponding to the first oxygen shell. This observation points toward a large reduction in the oxygen coordination number. The second effect is the shift of the main peak toward shorter distance, indicative of a shortening of the Cr−O bond. The positions of the framework phosphorus peaks corresponding to the small peak located at ca. 3.1 and 3.7 Å are accordingly shifted to shorter distance, as one would expect when the Cr−O bond in the Cr−O−P unit is shortened.

A detailed fitting of the data confirmed these preliminary observations (Figure 4 and Table 2), but also pointed out that the first main peak in the Fourier transformed spectra is in fact composed of two different oxygen shells that correspond to 3.1 O atoms at 1.89 Å plus 1.0 extra oxygen located at 2.33 Å giving a total coordination for O of 4.1 in the dehydrated sample. In contrast, for the hydrated CrAPO-5 sample a first coordination shell of 4.8 O at 1.96 Å was observed, while the second shell of 0.9 O was found at 2.39 Å. In this case, the total O coordination number was 5.7. Considering the uncertainty generally associated with the coordination numbers in EXAFS (10−20%), a coordination number close to 6 and 4 was found for hydrated and dehydrated CrAPO-5, respectively. The contraction of the first oxygen shell around Cr, which varies from 1.96 to 1.89 Å, and of the first P shell (3.23 to 3.13 Å) is also a strong argument in favor of a decrease in the coordination number. Indeed, as a general rule, the metal−O bond distance for the same metal oxidation state always increases as a function of the coordination number.[19] Moreover, as Cr^{3+} is replacing a framework Al^{3+}, it is connected to 4 P atoms via 4 O and the contraction of the Cr−O distance is consequently provoking the contraction of the Cr−P distances. The presence of one longer Cr−O bond in both dehydrated and hydrated CrAPO-5 and the relatively high Debye−Waller factor associated with this shell show that both tetrahedral and octahedral geometries of Cr^{3+} are largely distorted in microporous aluminophosphates. This longer bond can only be accounted for in the building of a structural model if the Cr atom slightly deviates from the normal Al position. The longer Cr−O bond is then connected to a P located at the surface of the next 12-ring pore in $AlPO_4$-5 molecular sieves (Figures 5 and 6). The two water molecules that complement the coordination to form a distorted octahedron are located in the channel of the porous solid. Although Cr−OH_2 distances are in general typically 1−2% longer than Cr−O distances,[19] this difference cannot be resolved by EXAFS, which gives a common average distance of 1.96 Å for the two Cr−OH_2 as for three of the four oxygen atoms connected to the framework. Plausible energy minimized structural models for a hydrated and dehydrated CrAPO-5 material are proposed in Figures 5 and 6.

In another set of X-ray absorption investigation experiments, a dehydrated CrAPO-5 material has been saturated with ammonia. The XANES region shows a centroid at around 5991.5 eV with intensity of about two-thirds of that of a fully dehydrated CrAPO-5 sample, located at 5992.1 eV. This intensity decrease is indicative of a deviation from the initial tetrahedral-like coordination; however, it does not point unambiguously toward a 6-fold coordination environment of Cr^{3+}. To confirm this observation, a detailed EXAFS analysis has been performed (Table 2). A good EXAFS fit was obtained when fitting the spectrum with three shells. Four oxygen or nitrogen atoms (EXAFS is not able to distinguish between both elements) are located at an average distance of about 1.94 Å; one oxygen or nitrogen atom is located at a longer distance of 2.40 Å, completing a 5-fold coordination environment. Although

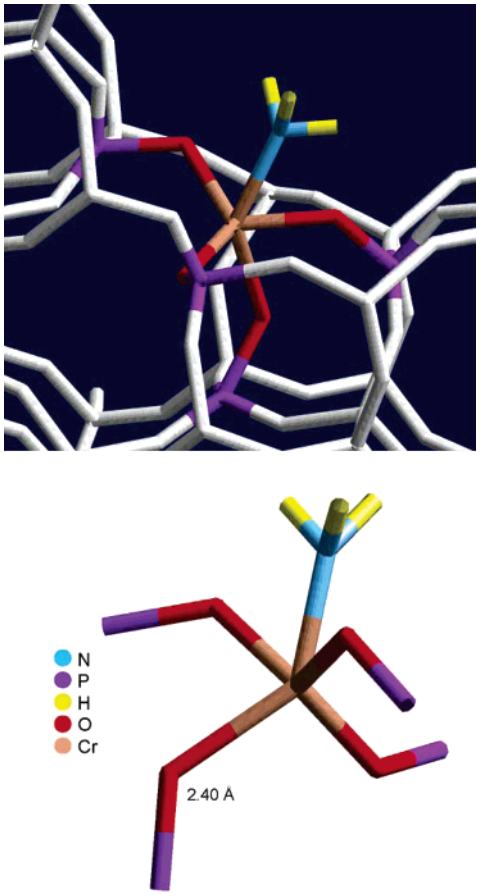

Figure 7. Proposed structural model for the local Cr coordination in ammonia saturated CrAPO-5.

typical Cr^{3+}−N bond distances (ca. 2.03 Å) are in general slightly longer than the corresponding Cr^{3+}−O ones (ca. 1.96 Å) in octahedral geometry,[19] it is difficult to predict accurately the Cr−N and Cr−O distances in such a mixed 5-fold coordination. Still, a reasonable structural model for an ammonia saturated CrAPO-5 material can be proposed (Figure 7).

Concluding Remarks

This XAFS investigation clearly shows that Cr^{3+} can be part of the framework of microporous crystalline AFI type aluminophosphate by replacing Al^{3+}. When the channels of the CrAPO-5 crystals are free of any adsorbates, the Cr^{3+} ions can exist in a distorted tetrahedral coordination, which is very unusual for Cr. Analysis of the XANES data (including a crystal field multiplet analysis) indicated that the formal oxidation state of the framework Cr ions remains 3+. Due to the $3d^3$ configuration of Cr^{3+}, the unusual coordination geometry of Cr^{3+} strongly tends to transform into the more stable 6-fold coordination by bonding two water molecules or into a 5-fold coordination by bonding one ammonia molecule. This characterization study also illustrates the versatility of transition metal ions to cope even with unfavorable coordination environments of a host, such as molecular sieves.

Acknowledgment. This work was supported by the Utrecht University XAFS user support group as well as by the NWO-VICI programme to B.M.W. The authors are grateful for beamtime at HASYLAB, E4 and for the help of Dr. K. Klementiev during the experiments. We also wish to acknowledge the use of the EPSRC's Chemical Database Service at Daresbury.

References and Notes

(1) (a) Ikeda, K.; Yagi, K. *Contrib. Mineral. Petrol.* **1977**, *61*, 91. (b) Ikeda, K.; Yagi, K. *Contrib. Mineral. Petrol.* **1982**, *81*, 113. (c) Schreiber, H. D. *Am. Mineral.* **1977**, *62*, 522. (d) Burns, R. G. *Geochim. Cosmochim. Acta* **1975**, *39*, 857.

(2) (a) Reinen, D. *Struct. Bonding* **1969**, *6*, 30. (b) Greenwood, N. N.; Earnshaw, A. *Chemistry of the Elements*; Pergamon Press: Oxford, UK, 1984. (c) Shriver, D. F.; Atkins, P. W.; Langford, C. H. *Inorganic Chemistry*, 2nd ed.; Oxford University Press: Oxford, UK, 1994. (d) Lever, A. B. P. *Inorganic Electronic Spectroscopy*, 2nd ed.; Elsevier: Amsterdam, The Netherlands, 1984.

(3) Burns, R. G. *Mineralogical Applications of Crystal Field Theory*, 2nd ed.; Cambridge University Press: Cambridge, UK, 1993.

(4) Brown, D. H. *J. Chem. Soc.* **1962**, *25*, 3322.

(5) (a) Doumerc, J. P.; Vlasse, M.; Pouchard, M.; Hagenmuller, P. *J. Solid State Chem.* **1975**, *13*, 275. (b) Doumerc, J. P.; Yangshu, W.; Dordor, P.; Marquestaut, E.; Pouchard, M.; Hagenmuller, P. *J. Phys. Chem. Solids* **1990**, *51*, 467.

(6) (a) Bottomley, F.; Chen, J.; MacIntosh, S. M.; Thompson, R. C. *Organometallics* **1991**, *10*, 906. (b) Allen, D. P.; Bottomley, F.; Day, R. W.; Decken, A.; Sanchez, V.; Summers, D. A.; Thompson, R. C. *Organometallics* **2001**, *20*, 1840.

(7) Sinha, K. P.; Sinha, A. P. B. *J. Phys. Chem.* **1957**, *61*, 758.

(8) Sunandana, C. S.; Phaninath, D. *Solid State Commun.* **1986**, *58*, 115.

(9) Some reviews on this subject: (a) Hartmann, M.; Kevan, L. *Chem. Rev.* **1999**, *99*, 635. (b) Weckhuysen, B. M.; Rao, R. R.; Martens, J. A.; Schoonheydt, R. A. *Eur. J. Inorg. Chem.* **1999**, 565. (c) Sheldon, R. A.; Wallau, M.; Arends, I. W. C. E.; Schuchardt, U. *Acc. Chem. Res.* **1998**, *31*, 485. (d) Thomas, J. M.; Raja, R.; Sankar, G.; Bell, R. G. *Acc. Chem. Res.* **2001**, *34*, 191. (e) Hartmann, M.; Kevan, L. *Res. Chem. Intermed.* **2002**, *28*, 625;

(10) Seminal examples on this subject: (a) Cora, F.; Sankar, G.; Catlow, C. R. A.; Thomas, J. M. *Chem. Commun.* **2002**, 734. (b) Thomas, J. M.; Raja, R.; Sankar, G.; Bell, R. G. *Nature* **1999**, *398*, 227. (c) Vanoppen, D. L.; De Vos, D. E.; Genet, M. J.; Rouxhet, P. G.; Jacobs, P. A., *Angew. Chem., Int. Ed. Engl.* **1995**, *34*, 560. (d) Weckhuysen, B. M.; Baetens, D.; Schoonheydt, R. A. *Angew. Chem., Int. Ed.* **2000**, *39*, 3419.

(11) (a) Davis, M. E.; Saldarriaga, C.; Montes, C.; Garces, J.; Crowder, C. *Nature* **1988**, *331*, 698. (b) Richardson, J. W.; Smith, J. V.; Pluth, J. J. *J. Phys. Chem.* **1989**, *93*, 8212. (c) McCusker, L. B.; Baerlocher, C.; Jahn, E.; Bulow, M. *Zeolites* **1991**, *11*, 308. (d) Peeters, M. P. J.; de Haan, J. W.; van de Ven, L. J. M.; van Hoof, J. H. C. *J. Chem. Soc., Chem. Commun.* **1992**, 1560. (e) Janchen J.; Peeters, M. P. J.; de Haan, J. W.; van de Ven, L. J. M.; van Hoof, J. H. C.; Girnus, I.; Lohse, U. *J. Phys. Chem.* **1993**, *97*, 12042.

(12) (a) Zhu, Z. D.; Wasowicz, T.; Kevan, L. *J. Phys. Chem. B* **1997**, *101*, 10763. (b) Zhu, Z. D.; Kevan, L. *Phys. Chem. Chem. Phys.* **1999**, *1*, 199. (c) Prakash, A. M.; Hartmann, M.; Zhu, Z. D.; Kevan, L. *J. Phys. Chem. B* **2000**, *104*, 1610. (d) Lempers, H. E. B.; Sheldon, R. A. *J. Catal.* **1998**, *75*, 62. (e) Radaev, S. F.; Joswig, W.; Baur, W. H. J. *Mater. Chem.* **1996**, *6*, 1413. (f) Miyake, M.; Uehara, H.; Suzuki, H.; Yao, Z. D.; Matsuda, M.; Sato, M. *Microporous Mesoporous Mater.* **1999**, *32*, 45. (g) Chen, J. D.; Lempers, H. E. B.; Sheldon, R. A. *J. Chem. Soc., Faraday Trans.* **1996**, *92*, 1807. (h) Buijs, W.; Raja, R.; Thomas, J. M.; Wolters, W. *Catal. Lett.* **2003**, *91*, 253.

(13) (a) Weckhuysen, B. M.; Schoonheydt, R. A. *Zeolites* **1994**, *14*, 360. (b) Weckhuysen, B. M.; Schoonheydt, R. A. *Stud. Surf. Sci. Catal.* **1994**, *14*, 360. (c) Weckhuysen, B. M.; Schoonheydt, R. A.; Mabbs, F. E.; Collison, D. *J. Chem. Soc., Faraday Trans.* **1996**, *92*, 2431. (d) Rajic, N.; Stojakovic, D.; Hocevar, S.; Kaucic, V. *Zeolites* **1993**, *13*, 384. (e) Demuth, D.; Unger, K. K.; Schuth, F.; Stucky, G. D.; Srdanov, V. I. *Adv. Mater.* **1994**, *6*, 931. (f) Demuth, D.; Unger, K. K.; Schuth, F.; Srdanov, V. I.; Stucky, G. D. *J. Phys. Chem.* **1995**, *99*, 479. (g) Thiele, S.; Hoffman, K.; Vetter, R.; Marlow, F.; Radaev, S. *Zeolites* **1997**, *19*, 190.

(14) (a) Kornatowski, J.; Zadrozna, G.; Wloch, J.; Rozwadowski, M. *Langmuir* **1999**, *15*, 5863. (b) Padlyak, B. V.; Kornatowski, J.; Zadrozna, G.; Rozwadowski, M.; Gutsze, A. *J. Phys. Chem. A* **2000**, *104*, 11837. (c) Kornatowski, J.; Zadrozna, G.; Rozwadowski, M.; Zibrowius, B.; Marlow, F.; Lercher, J. A. *Chem. Mater.* **2001**, *13*, 4447. (d) Zadrozna, G.; Souvage, E.; Kornatowski, J. *J. Catal.* **2002**, *208*, 270.

(15) (a) Weckhuysen, B. M.; Wachs, I. E.; Schoonheydt, R. A. *Chem. Rev.* **1996**, *96*, 3327. (b) Groppo, E.; Lamberti, C.; Bordiga, S.; Spoto, G.; Zecchina, A. *Chem. Rev.* **2005**, *105*, 115.

(16) (a) Peterson, M. L.; Brown, G. E.; Parks, G. A.; Martin, F. *Geochim. Cosmochim. Acta* **1997**, *61*, 3399. (b) Pandya, K. I. *Phys. Rev. B* **1994**, *50*, 15509. (c) Groppo, E.;, Prestipino, C.; Cesano, F.; Bonino, F.; Bordiga, S.; Lamberti, C.; Thune, P. C.; Niemantsverdriet, J. W.; Zecchina, A. *J. Catal.* **2005**, *230*, 98.

(17) (a) Wilke, M.; Farges, F.; Petit, P. E.; Brown, G. E.; Martin, F. *Am. Mineral.* **2001**, *86*, 714. (b) Wong, F.; Lytle, J. W. P. M. R.; Maylotte, D. H. *Phys. Rev. B* **1984**, *30*, 5596. (c) Heijboer, W. M.; Glatzel, P.; Sawant, K. R.; Lobo, R. F.; Bergmann, U.; Barrea, R. A.; Koningsberger, D. C.; Weckhuysen, B. M.; de Groot, F. M. F. *J. Phys. Chem. B* **2004**, *108*, 10002.

(18) Binsted, N.; Gurman, S. J.; Stephenson, P. C. *EXAFS Analysis Programs*; Daresbury Laboratory: Warrington, UK, 1991.

(19) (a) de Groot, F. M. F. *J. Electron Spectrosc.* **1994**, *67*, 529. (b) de Groot, F. *Coord. Chem. Rev.* **2005**, *249*, 31.

(20) Fletcher, D. A.; McMeeking, R. F.; Parkin, D. *J. Chem. Inf. Comput. Sci.* **1996**, *36*, 746.

(21) Klap, G. J.; van Koningsveld, H.; Graafsma, H.; Schreurs, A. M. M. *Microporous Mesoporous Mater.* **2000**, *38*, 403.